




Rainwater geochemistry inside the Barcarena power station at the mouth of the Tocantins River

Darilena Monteiro Porfírio, Lucilena Rebêlo Monteiro & Marcondes Lima da Costa


To cite this article: Darilena Monteiro Porfírio, Lucilena Rebêlo Monteiro & Marcondes Lima da Costa (2018): Rainwater geochemistry inside the Barcarena power station at the mouth of the Tocantins River, Environmental Technology, DOI: [10.1080/09593330.2018.1516801](https://doi.org/10.1080/09593330.2018.1516801)

To link to this article: <https://doi.org/10.1080/09593330.2018.1516801>

 View supplementary material [↗](#)

 Accepted author version posted online: 27 Aug 2018.
Published online: 19 Sep 2018.

 Submit your article to this journal [↗](#)

 Article views: 57

 View Crossmark data [↗](#)



Rainwater geochemistry inside the Barcarena power station at the mouth of the Tocantins River

Darilena Monteiro Porfírio ^{a,b}, Lucilena Rebêlo Monteiro ^c and Marcondes Lima da Costa ^b

^aCentro de Tecnologia da Eletronorte Eletrobrás (OCT), Belém, Brasil; ^bPrograma de pós-graduação em Geologia e Geoquímica da Universidade Federal do Pará (PPGG-UFGPA), Belém, Brasil; ^cIpen/CNEN-SP – Instituto de Pesquisas Energéticas e Nucleares, São Paulo, Brasil

ABSTRACT

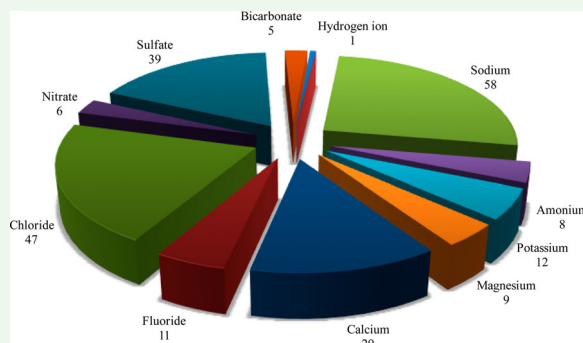
Most of South America lacks studies on rainwater composition. The present study evaluates rainwater composition and bulk deposition inside Barcarena power station, located at the mouth of the Tocantins River with Amazon River in Brazil. In 2012, 24-h rainwater samples were collected inside the ELETRONORTE power plant ($n = 93$), and pH, EC, cations and anions were analyzed. In order of abundance, the rainwater ions were $\text{Na}^+ > \text{Cl}^- > \text{SO}_4^{2-} > \text{Ca}^{+2} > \text{K}^+ > \text{F}^- > \text{Mg}^{+2} > \text{NH}_4^+-\text{N} > \text{NO}_3^--\text{N}$. pH values ranged from 4.5 to 6.9, with 17 events with pH < 5.6 and 5 events with pH < 5.0 . Sodium and Cl^- were the dominant ions with sea salt as main contribution. Acidity, enrichment factors and principal component analysis (PCA) indicate that F^- , SO_4^{2-} and NO_3^--N in the rainwater came from anthropogenic sources. Fluoride correlated strongly (> 0.85) with Ca^{+2} and Mg^{+2} , likely originated from same source in the aluminum production chain. Potassium originated from a mixture of anthropogenic and natural sources, with a good correlation (> 0.70) with NO_3^--N and NH_4^+-N , indicating biomass burning and fertilizer origins. In 2012, Barcarena total bulk deposition ranged from 14,070 to 17,890 $\text{mg m}^{-2} \text{y}^{-1}$ with significant contributions of SO_4^{2-} (2,385 to 2,851 $\text{mg m}^{-2} \text{y}^{-1}$), F^- (419 to 479 $\text{mg m}^{-2} \text{y}^{-1}$) and NO_3^--N (128 to 280 $\text{mg m}^{-2} \text{y}^{-1}$). EC values (4 to 254 $\mu\text{S cm}^{-1}$) indicated a medium site pollution severity ($> 175 \mu\text{S cm}^{-1}$), which increased the risk of damage to electrical components.

ARTICLE HISTORY

Received 26 December 2017
Accepted 20 August 2018

KEYWORDS

Rainwater and pollution; enrichment factor; major ions; power plant; principal component analysis





Highlights


- Chemical characterization of Barcarena, PA/Brazil rainwater in 2012 events.
- Apportionment sources of ionic rainwater content evaluated by acidity fraction, enrichment factors and principal component analysis.
- Anthropogenic fluoride, sulfate and nitrate local deposition values were compared with other regional data.
- Maintenance procedure recommendations under identified atmospheric deposition.

1. Introduction

Rainwater is the most effective scavenging factor that cleans the air. For this reason, rainwater studies can be used to help understand local and regional pollutant dispersion [1]. Many places worldwide have continuous

long-term rainwater monitoring records that allow the identification of changing trends. However, most South America countries have no continuous or available data on the geochemical composition of rainwater or ion deposition rates. Studies on deposition rates close to

CONTACT Darilena Monteiro Porfírio  darilenap@yahoo.com.br  Centro de Tecnologia da Eletronorte Eletrobrás (OCT), Belém, PA CEP 66115-000, Brasil; Programa de pós-graduação em Geologia e Geoquímica da Universidade Federal do Pará (PPGG-UFGPA), Belém, PA, Brasil

 Supplemental data for this article can be accessed at <https://doi.org/10.1080/09593330.2018.1516801>.

© 2018 Informa UK Limited, trading as Taylor & Francis Group

industrial parks and urban areas demand yearlong continuous sample collection.

In urban and industrial scenarios, dust particles coming from several sources (natural and anthropogenic) increase the atmospheric ion content. Aerosols generated through processes such as gas to particulate conversion in industrial emissions, wind erosion of sediments and soils, and the production of large quantities of organic and inorganic smoke particles from fires can mix with natural marine aerosols and volcanic emissions [2]. Due to elevated rainwater ion contents, several urban coastal industrial areas worldwide experience high frequencies of electrical component failure. In a study performed on the island of Crete, Pylarinos et al. [3] linked the failure of open-air high voltage insulators to environmental conditions, especially air pollution. Environmental data from France, Germany, Poland and Algeria reveal that high-voltage insulator failure is related to industrial air contamination trends (dust, SO_2 , NO_x , acidity and rainwater conductivity) [4]. Airborne particulate matter and ionic compounds after condensation (rainout) and precipitation (washout) directly affect insulator sets. Due to this observation, insulators are considered the typical failing components. A conductive film commonly forms on insulators due to sources of humidity, which, when the ion content is sufficiently high, leads to current leakage. The formation of a saline band favors discharges and flashover conditions. Therefore, urban and industrial air pollutants directly threaten electrical components.

In the North Region of Brazil, the Tucuruí Dam hydropower station is responsible for a yearly production of 8,700 MW, which corresponds to 10% of Brazil's electrical power demand. The Barcarena power station is connected to a total of 328 km of transmission lines and has a distribution capacity of 325 kWh [5]. In 1985, managed by Centrais Elétricas do Norte do Brasil S.A. (ELETRONORTE), the Tucuruí Dam hydropower station started operation. Since Tucuruí was connected to the Vila do Conde power station, several power-intensive industries, fertilizer manufacturers and ore mineral processing companies developed in Barcarena. In 2016, Barcarena was the 13th most populated and the 5th highest gross domestic product (GDP) city in Para state [6]. The GDP position is related to a busy harbour and a variety of industrial activities located in Barcarena. According to dos Santos [7], Barcarena currently has a yearly installed capacity of 3,452 MW that is supplied to 2.6 million inhabitants [6].

In 1995, the largest alumina refinery in the world started operation in Barcarena 4.7 km far from the present study collection site. After three expansions, the alumina production reached a value of approximately 6

million metric ton (t), which is then processed in smelters around the world [8]. In 2016, this production facility was Brazil's second largest, with a yearly primary aluminum production of 460,000 t [8]. Although atmospheric emissions are regulated and limited, the aluminum company declared a total worldwide fluoride emission to air of 507 t in 2012 [9]. However, no clear statement is available about atmospheric fluoride emissions in Barcarena during the operational years.

Following the expansion of the industrial centre, the ELETRONORTE maintenance team observed insulator corrosion, electrical component failure and vegetation damage that could be linked to precipitation and atmospheric events. No previous study has identified the source of the frequent failure events in Barcarena. Many influential aspects in the present study have strictly local characteristics due to the industrial surroundings. However, the Barcarena rainwater chemical composition, ion deposition rates and enrichment factors were not available until now. These relevant parameters are required to understand atmospheric scavenging and to improve preventive maintenance of electrical components.

Conducted in 2012 inside the ELETRONORTE power station, the present study primarily seeks to identify the major ions in Barcarena rainwater and the deposition rates of these ions. This information will help to improve transmission line maintenance and economic performance.

2. Material and methods

2.1. Study area

Rainwater samples were collected in a single site, in the area inside ELETRONORTE power station located at Barcarena (1°34'17" S and 48°44'2" W). Barcarena is located in Ponta Grossa, in eastern Para, at the confluence of the large Tocantins and Guamá Rivers [10], as shown in Figure 1. The Atlantic Ocean is 142 km north-east of the collection site.

Barcarena County covers an area of 1,310 km² and has 118,537 inhabitants [6]. The climate of Barcarena is typically tropical, hot, and wet with an average temperature of $26.9 \pm 0.8^\circ\text{C}$ and a total annual rainfall of 2,532 mm. The temperature amplitude is quite narrow, and the humidity is over 90%. The majority of the precipitation occurs from December to June, during the rainy or winter season, and March features the largest monthly precipitation amount, with a historical average rainfall of 387 mm from 1961 to 1990 [11]. The often-called dry season extends from July to November, and November features the lowest monthly precipitation, (<80 mm). The monthly precipitation average is 211 mm [11].

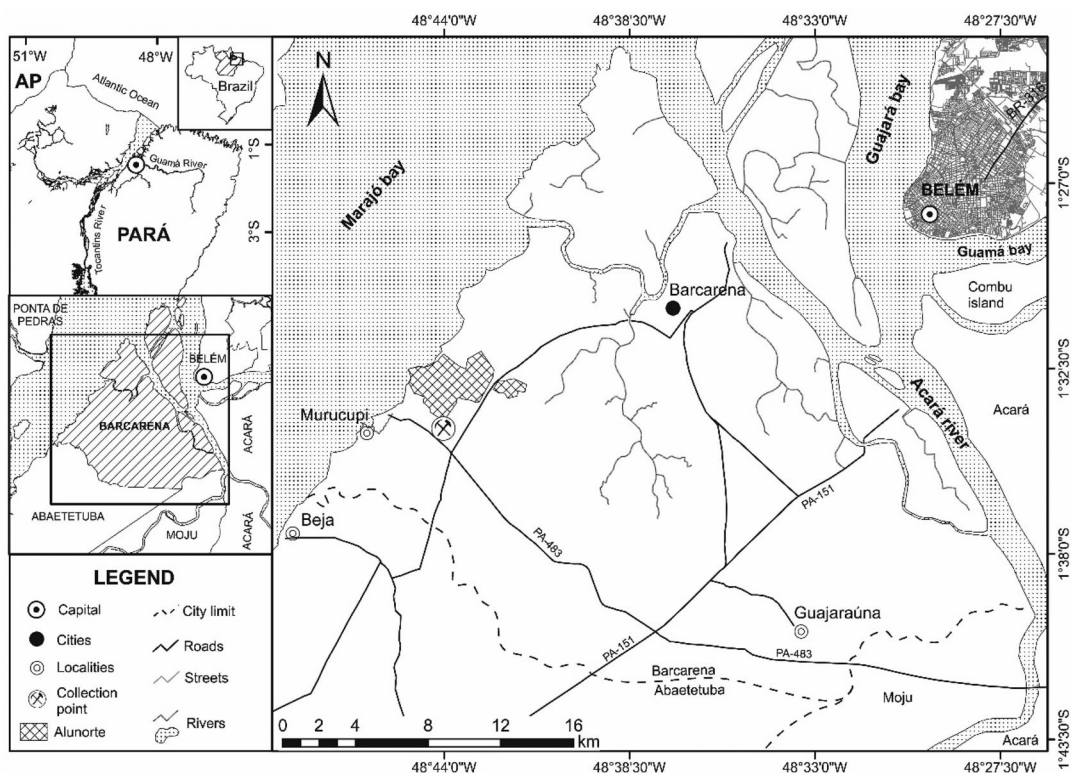


Figure 1. Geographic location of the sampling site.

According to SATYAMURTY et al., Amazonian Basin humidity sources are located in the South and North Atlantic, in the so-called Intertropical Convergence Zone (ICZ) [12]. The ICZ transports the humidity that feeds the Amazonian Basin from east to west all year long. The precipitation recycled by evapotranspiration is estimated to be approximately 33% in the rainy season, with smaller values in the dry season.

The predominant wind direction shifts from northwest to northeast during the nighttime and from northeast to northwest during the daytime. There are no heavy traffic roads nearby, and the roads with the heaviest traffic are BR-010, located 85 km northeast of the collection site, and PA-151 and its connections, located southeast of the collection site. Regionally, Barcarena County is located on the Amazon plain and is bounded by Marajo and Guajara Bays to the north, Moju and Abaetetuba Counties to the south, Acara and Guajara Bays to the east, and the Tocantins River and Marajo Bay to the west [13], as presented in Figure 1.

2.2. Rainwater sampling and analysis

From January 2012 to January 2013, at the single collection site (see Figure 1), a total 93 rainwater events were collected for this study. A minimum volume of 5 mL was required. Each event corresponded to 24 h bulk

pluvial samples collected from 10am to 10am to the next day as recommended by the World Meteorological Organization – WMO [14]. Polypropylene bottles and funnels were used as sample collection sets. Ultrapurified water (18 M Ω , Milli-Q, Millipore) was used to rinse and clean all samplers prior to each collection. During every collection, the sampler was placed 5 m above local ground level, which is 15 m above sea level. The collection area, i.e. the funnel area, was 0.0165 m². This value was later used in the deposition calculation.

By this procedure, both dry and wet deposition samples were collected together and reported as bulk sample collection [14]. The total sample volume was measured, and the samples were cooled and sent to the laboratory weekly. The registered volume values were used later to calculate the volume-weighted mean (VWM) ion concentration. This type of calculation is required [14,15] to correct for the individual precipitation volume, which differs among all events and affects individual ion concentrations.

At the laboratory, all samples were filtered through a 0.45 μ m membrane. Field and filtration blanks were treated the same as samples. Physical and chemical parameters, such as pH [16], conductivity (EC) [17], and concentrations of cations (Na⁺, K⁺, Ca⁺², Mg⁺², NH₄⁺) [18] and anions (F⁻, Cl⁻, NO₃⁻, SO₄⁻², PO₄⁻³) [19], were measured.

For the samples, pH was measured with a potentiometer (QUIMIS, Q400-A) calibrated with pH 4.00 and 7.00 standard buffer solutions (VETEC). Bicarbonate and H^+ were not directly measured but accounted as per pH basis, as recommended by the Canadian government in Alberta [20]. Conductivity was measured with a conductivity cell (DIGIMED, DM-32), which was calibrated with $1,413 \mu\text{Scm}^{-1}$ (Hanna Instruments, model HI7031). A dual-channel ICS5000 ion chromatographer (DIONEX Corp.) with a simultaneous electrochemical auto-regenerative suppression conductivity detector was used in the anion and cation analysis. Methanesulfonic acid (20 mm) was the cation separation eluent in the isocratic elution, and potassium hydroxide (5–40 mm for 30 min) was the gradient anion separation eluent. The method quantification limits varied from 1 to $5 \mu\text{eq L}^{-1}$ among quantified compounds and from 6 to $9 \mu\text{eq L}^{-1}$ for non-detected species. Gradient elution for anions was required to achieve fluoride separation from acetate, formate and propionate, which were present in the bulk samples.

2.3. Analysis quality control

All chromatographic analysis included a daily blank, duplicate runs and three levels of standard quality control verification. A deviation of no more than 2% from the expected concentration was allowed. Monthly, the laboratory performed a full calibration, where variation of no more than 5% was found for all cations and anions over 12 months. The results were converted to SI units by using DIONEX standard solutions and standard weights. The laboratory participates regularly in interlaboratory exercises for pH, cation and anion measurements with satisfactory results for all measured parameters [21]. Data quality control followed WMO recommendation concerning laboratory data verification, reporting, ionic balance and acceptance criteria of $\pm 60\%$, $\pm 30\%$, $\pm 15\%$ and $\pm 10\%$ acceptable ion differences for samples with anion and cation sums of $\leq 50 \mu\text{eq L}^{-1}$, >50 to $\leq 100 \mu\text{eq L}^{-1}$, >100 to $\leq 500 \mu\text{eq L}^{-1}$ and $>500 \mu\text{eq L}^{-1}$, respectively [14].

2.4. Statistical data treatment

The programme PAST (Paleontological Statistics version 3.14 from the Natural History Museum of Oslo University) was used to perform statistical treatments on all the data in order to evaluate the origins of the major ions [22]. Multivariate data analysis was performed on a matrix with 93 cases or events and 14 variables or parameters. Principal component analysis (PCA) was used to identify and to group parameters that explain the matrix

variability. However, monthly and seasonal evaluations were adopted to present and discuss other data treatments (sections 3.1–3.6). The effects of asymmetric rainfall distribution are minimized due to tropical conditions (intense and frequent precipitation events of <100 mm per month), so we adopt the monthly and seasonal discussion according to VAREJÃO-SILVA [23]. Several authors adopted similar models, such as HU, BALASUBRAMANIAN, WU and XIAO [24,25].

2.5. Fractional acidity, ion to ion ratios and enrichment factor

In this work, rainwater capacity of acidity neutralization was estimated as fractional acidity (FA) [25], presented in equation 1.

$$FA = [H^+]/([NO_3^-] + [SO_4^{2-}]_{NSS}) \quad (1)$$

where

$[H^+]$ is the hydronium concentration calculated from pH

$[NO_3^-]$ is the nitrate concentration in the rainwater

$[SO_4^{2-}]_{NSS}$ is the non-sea salt sulfate concentration in the rainwater

When FA is close to 1, the rainwater acidity is considered to be generated by SO_4^{2-} and NO_3^- .

Neutralization factors (NFs) were also calculated on the basis of equation 2.

$$NF_x = [X]/([NO_3^-] + [SO_4^{2-}]_{NSS}) \quad (2)$$

where $[X]$ is the ion of interest.

The ratios of major ions to sodium and to calcium in Barcelona rainwater, as well as enrichment factors (EFs), were calculated. Often, an EF is used to identify possible rainwater ion sources, especially to determine whether anion and cation species came from sea salt, from continental crust or from anthropogenic origins [24,25]. Several researchers [24–28] have used this approach to clarify the sources that contribute rainwater ion species. In this work, Na^+ was considered the reference element for seawater and was assumed to be of purely marine origin, while Ca^{2+} was assumed to be a proxy for rocks and represented the reference element for continental crust and soil.

The EFs were calculated as presented in equations 3 and 4 [24,25].

$$EF_{(seawater)} = [x]/[Na^+]_{(rainwater)}/[x]/[Na^+]_{(seawater)} \quad (3)$$

$$EF_{(crust)} = [x]/[Ca^{2+}]_{(rainwater)}/[x]/[Ca^{2+}]_{(crust)} \quad (4)$$

where $[x]$ is the chemical component of interest in $\mu\text{g L}^{-1}$ either in rainwater or in seawater;

$[Na^+]_{(rainwater)}$ is sodium in $\mu\text{g L}^{-1}$ present in the rainwater in this study.

$[\text{Ca}^{2+}]_{(\text{rainwater})}$ is calcium in $\mu\text{g L}^{-1}$ present in the rainwater in this study.

$[\text{Na}^+]_{(\text{seawater})}$ is the sodium reference concentration in $\mu\text{g L}^{-1}$ in seawater.

$[\text{Ca}^{2+}]_{(\text{crust})}$ is the calcium reference in $\mu\text{g L}^{-1}$ in crustal components.

The sea salt factor (SSF), crustal factor (CF) and anthropogenic factor (AF) were calculated with equations 5, 6 and 7 [24–28].

$$\%SSF = 100 \cdot [x]/[\text{Na}^+]_{(\text{seawater})} / [x]/[\text{Na}^+]_{(\text{rainwater})} \quad (5)$$

$$\%CF = 100 \cdot [x]/[\text{Ca}^{2+}]_{(\text{crust})} / [x]/[\text{Ca}^{2+}]_{(\text{rainwater})} \quad (6)$$

$$\%AF = 100 - (\%SSF + \%CF) \quad (7)$$

The amount of sodium in samples was also used as a marine tracer that enabled us to distinguish between the sulfate fraction from sea spray (SS) and that from non-sea salt sources (NSS) [29,30] as per equation 8.

$$[\text{SO}_4^{-2}]_{\text{NSS}} = [\text{SO}_4^{-2}]_{\text{total}} - 0.12041 \times [\text{Na}^+] \quad (8)$$

where $[\text{SO}_4^{-2}]_{\text{total}}$ is the total sulfate concentration;

$[\text{SO}_4^{-2}]_{\text{NSS}}$ is the non-sea salt sulfate concentration;

$[\text{Na}^+]$ is the sodium concentration in the sample;

and the ratio between the concentrations of SO_4^{-2} and Na^+ (in $\mu\text{eq L}^{-1}$) in seawater is 0.12041.

2.6. Bulk deposition

Bulk deposition (in $\text{mg m}^2 \text{day}^{-1}$) was obtained by multiplying the compound VWM concentration in the samples [X] in mg L^{-1} by the rainfall in L day^{-1} , which is calculated based on the volume of rainwater collected over an area of 0.0165 m^2 . Bulk precipitation was chosen

over wet-only and dry deposition. Wet-only deposition is considered to approximately represent long-term trends, as stated by LAJTHA et al., but is prone to underestimation of cation inputs in dusty areas and commonly yields lower total inputs [4]. On the other hand, dry-only deposition was considered not compatible with the local rainy, high-humidity tropical climate. Therefore, bulk precipitation was considered the most suitable for performing the source apportionment.

The collected samples and all corresponding data should be considered local, according to the WMO classification, due the collection site's short distance to cities, roads and industrial complexes. In this work, bulk precipitation needs to be associated with a WMO warning that an unknown amount of dry matter due to dry weather deposition could be involved [14]. Both maximum and minimum bulk deposition values were separately calculated. The maximum deposition ($\text{mg m}^{-2} \text{y}^{-1}$) was calculated considering annual precipitation depth and precipitation weighted mean for all validated events. The minimum deposition was calculated considering all individual daily precipitation events relative to all validated and non-null events [14,20]. The difference between the maximum and minimum deposition values is derived from the data completeness that should accompany the data for further comparison (see section 3.8).

3. Results

3.1. Rain quantity

Figure 2 presents monthly rainfall during the sampling period compared with Barcarena historical average

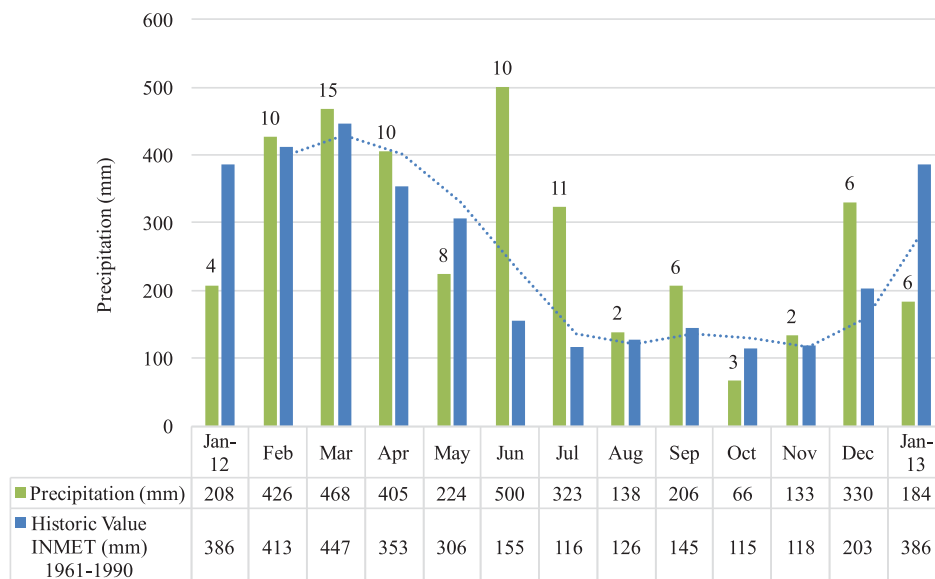


Figure 2. Monthly rainfall and monthly precipitation events from January 2012 to January 2013.

rainfall from 1961 to 1990 and the monthly number of precipitation events. In this work, a 24-hour collection interval in which more than 5 mL of rain was collected was considered one single precipitation event. The highest number of precipitation events was observed during March ($n = 15$), followed by July (11) and February, April, and June (10). The lowest number of precipitation events occurred in November (2), August (2), October (3) and January 2012 (4). The monthly average and yearly total rainfall during the study period were 278 mm and 3,404 mm respectively. The yearly total is approximately 500 mm over the historical annual average of 2,900 mm [11] in the study area. However, this high precipitation value is compatible with the region's hot and wet tropical climate and to decennial historical records. In June, July, September and December 2012, the measured precipitation exceeded historical values (Figure 2). In contrast, in January, May and October 2012 and January 2013, the precipitation was below the historical average. The precipitation in February, March, April, August and November 2012 was similar to the expected historical average. High monthly averages were observed in 2012 from February to July. Overall, precipitation during these months corresponded to 68.9% of the yearly total rainfall measured in this study. The dry season was relatively short from August to November 2012, with the next rainy season starting in December 2012. Short dry seasons can lead to lower dust occurrence as well as lower ion concentrations. Future concentration comparisons must consider seasonal changes or refer directly to yearly bulk deposition values to overcome seasonal influences.

3.2. pH and conductivity

The rainwater pH values ranged from 4.52 to 6.96, and the EC values varied from 4 to 254 $\mu\text{S cm}^{-1}$ ($n = 93$). Monthly pH and conductivity VWM values are presented in Figure 3. During the year, pH showed a slight variation ($\text{SD} = 0.41$). Only 17 events presented values lower than 5.6, which is the usual reference pH value for rainwater in undisturbed equilibrium with atmospheric CO_2 . In rainwater samples with $\text{pH} \geq 5.6$, no significant effects from NO_x , SO_x or other acidic species were observed. Low conductivity values were observed during the wet season, showing the atmosphere cleaning process and dilution effect that are usually observed during this period. The EC values were highest in August, October and December 2012, as months correspond to the dry season. No statistically significant difference was observed in pH and CE values between the rainy season (5.8 ± 0.4 and $22 \pm 19 \mu\text{S cm}^{-1}$) and the dry season (5.9 ± 0.4 and $35 \pm 20 \mu\text{S cm}^{-1}$), with annual average values of 5.9 ± 0.4 and $15 \pm 15 \mu\text{S cm}^{-1}$ for pH and conductivity, respectively, as presented in Table 1.

Considering rainwater samples with $\text{pH} \leq 5.6$, increases of approximately 45% in SO_4^{2-} , F^- , NH_4^+ and NO_3^- -N, and increases of 20%–37% in Na^+ , Mg^{+2} , Ca^{+2} and Cl^- were observed in these samples relative to all sample data. Low pH values (≤ 5.0) were observed in only 5 events. Among these low-pH events, SO_4^- increased significantly (over 200%) relative to the whole sample set. In the same 5 events, the remaining ions, such as F^- , NO_3^- -N, Na^+ , Mg^{+2} and Cl^- , increased by its values in a range from 79% up to 115%. These issues are discussed further with EFs and source

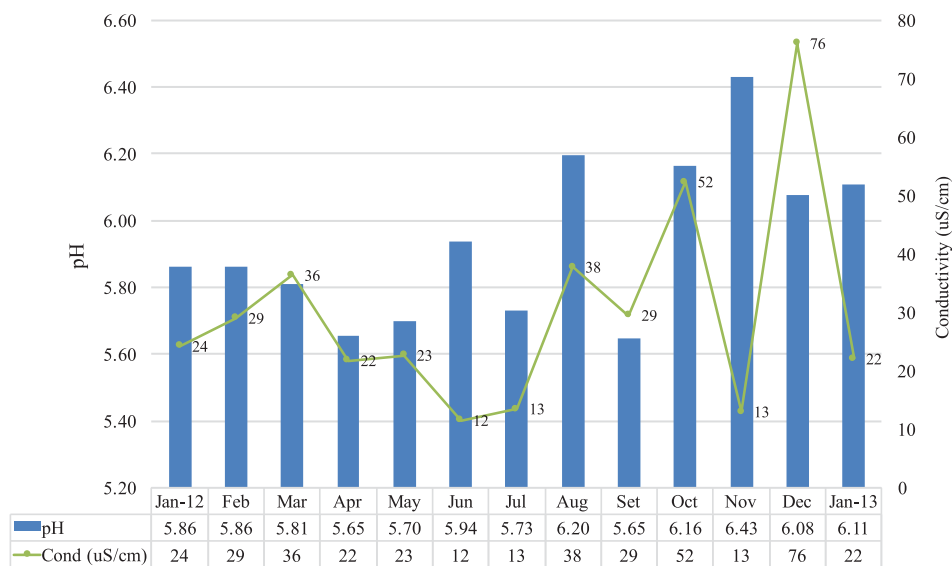


Figure 3. pH and conductivity VWM in Barcarena rainwater.

Table 1. Annual VWM of pH, EC ($\mu\text{S cm}^{-1}$), H^+ , major cation and anion concentrations and totals ($\mu\text{eq L}^{-1}$).

Parameter	VWM	sd	max	min	Arithmetic mean	sd	max	Min
pH	5.9	0.4	7.0	5.1	5.9	0.4	7.0	5.1
EC	15	15	88	2.1	29	34	254	4
H^+	1.2	0.4	6.4	0.0	1.2	0.4	2.5	0.4
Na^+	58	68	352	5	129	213	1367	<5*
NH_4^+	8	24	166	<3*	16	41	267	<3*
K^+	12	58	50	<3*	18	42	245	<3*
Mg^{+2}	9	16	80	<1*	20	42	244	<1*
Ca^{+2}	29	30	120	<2*	56	87	663	<2*
F^-	11	17	115	<1*	24	39	250	<1*
Cl^-	47	49	243	7	94	151	1062	3
$\text{NO}_3^- \text{N}$	6	9	33	<3*	10	20	165	<3*
SO_4^{-2}	39	43	236	<1*	72	96	569	<1*
$\text{SO}_4^{-2} \text{NSS}$	34	38	207	0	63	84	501	0
HCO_3^-	4.9	5.9	28.6	0.1	5.0	1.9	13.3	2.0
Sum anion	104	113	684	7	193	233	1740	3
Sum cation	110	114	668	5	218	293	2330	1

*Quantification limit.

**Sum anions includes bicarbonate values obtained by equilibrium data [20].

apportionment. No alkaline values were observed in any of the 93 monitored events.

3.3. Major ion contents

The annual VWM concentrations of the major anions ($\mu\text{eq L}^{-1}$) in rainwater from January 2012 to January 2013 are presented in Table 1. An arithmetic mean concentration that is higher than the median indicates asymmetry in the frequency distribution due to higher concentration values. The VWM was smaller than the arithmetic mean, as usually observed in rainwater samples. The adoption of VWM values corrects any skewed values due to lower or higher precipitation events, as described by Xiao [25]. No contents of Li^+ , Br^- , $\text{NO}_2^- \text{N}$ and $\text{PO}_3^- \text{P}$ above the quantification limits were detected in Barcarena rainwater (6, 9, 9 and $0.5 \mu\text{eq L}^{-1}$, respectively). Among the 93 events, 10 were considered outliers according to the

ionic balance criteria of the WMO and excluded from the data set [14]. These outliers could indicate unnoticed contamination by pollen, insects or microorganisms or indeed rainwater disturbances caused by isolated anthropogenic sources. An odd frequency of 8 of the 10 outliers occurred on Tuesdays and Fridays from January to July. Hence, external event interference could be to blame and requires further elucidation (see supplementary material).

Despite the unaccounted anions, the data presented a good balance between anions and cations, where $\sum \text{anions} / \sum \text{cations} = 0.6758$, indicating that the major ions have been well measured (see Figure 4). The majority of events had concentrations below $150 \mu\text{eq L}^{-1}$ for cations (60%) and anions (65%). No more than 6 events were above $300 \mu\text{eq L}^{-1}$ for both cations and anions. These high concentration events could contribute to degradation of insulators, metallic

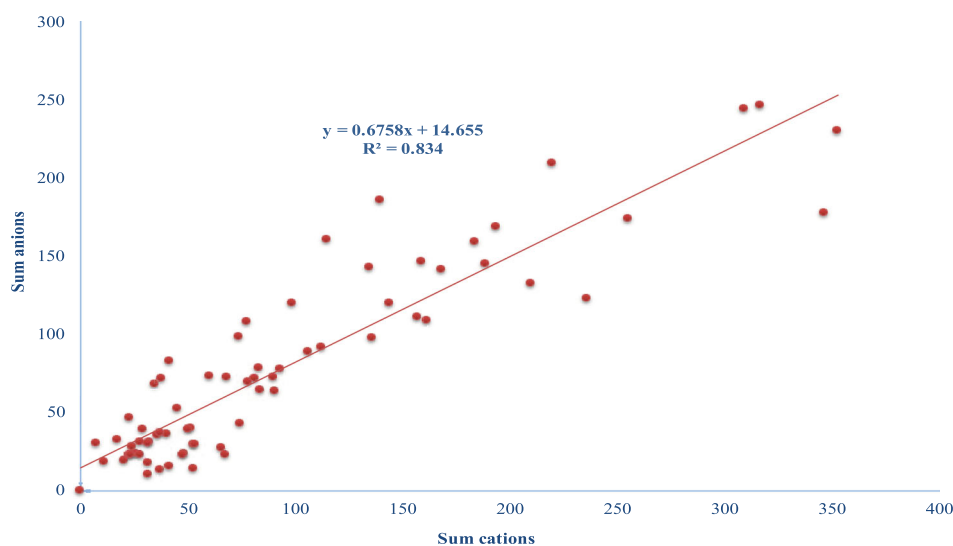


Figure 4. Total cations against total anions, in $\mu\text{eq L}^{-1}$.

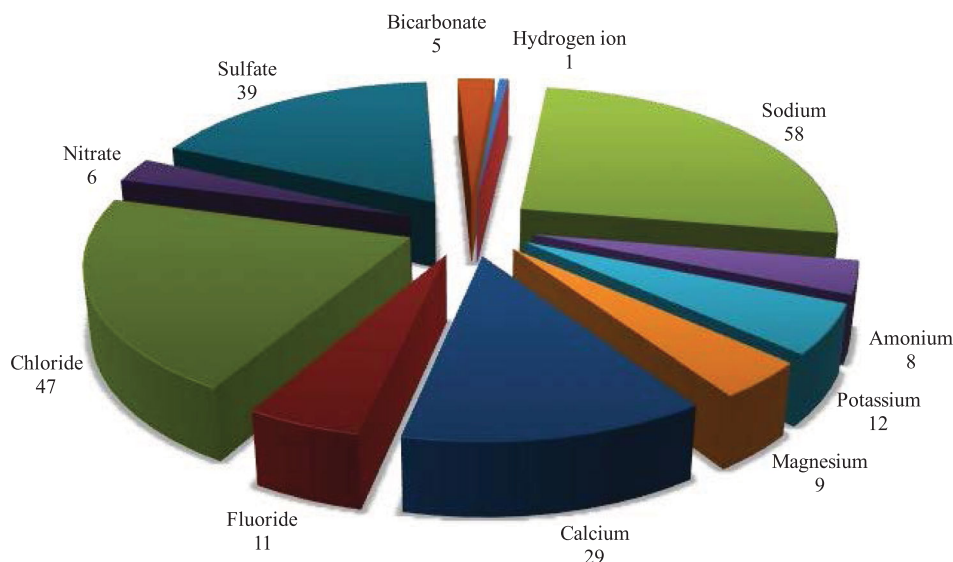


Figure 5. Annual cation and anion VWM concentrations ($\mu\text{eq L}^{-1}$) in Barcarena rainwater.

pins and ceramic surfaces [31]. Elevated EC values in rain and fog increases insulator surface contamination and decreases flashover voltage [32].

The one-year cation and anion sum VWM \pm sd values were $110 \pm 114 \mu\text{eq L}^{-1}$ and $104 \pm 113 \mu\text{eq L}^{-1}$, respectively, with large dispersion around the average, indicating considerable variation in the ion content. These values were compatible with the wet-only long-term average ion concentrations in countries like Spain, Russia, France, Sweden and Switzerland after 1990 and the Clean Air Act Amendments and were much lower than values found in the Netherland, Great Britain, Poland, Norway, Germany and Austria, [4].

In order of annual VWM abundance, the ions in Barcarena rainwater in decreasing order were $\text{Na}^+ > \text{Cl}^- > \text{SO}_4^{2-} > \text{Ca}^{+2} > \text{K}^+ > \text{F}^- > \text{NH}_4^+ > \text{Mg}^{+2} > \text{NO}_3^- \text{-N}$, as presented in Figure 5. Chloride ($47 \mu\text{eq L}^{-1}$) and sulfate ($39 \mu\text{eq L}^{-1}$) were the most abundant anions and were present in 100% of precipitation events. The most abundant cations by VWM were sodium ($58 \mu\text{eq L}^{-1}$) and calcium ($29 \mu\text{eq L}^{-1}$). Both cations were present in 100% of events (see Figure 5).

Potassium, Mg^{+2} and NH_4^+ were less frequent, occurring in 61%, 46% and 14% of events, respectively, with VWM values of $12 \mu\text{eq L}^{-1}$, $9 \mu\text{eq L}^{-1}$ and $8 \mu\text{eq L}^{-1}$, respectively. Among the cations, Na^+ , Ca^{+2} , Mg^{+2} and K^+ (base cations) can originate from sea salt, dust, biomass burning, industrial emissions, particulate matter from road and off-road dust and vehicle emissions [32]. Calcium is considered as a proxy for basic particles that neutralize acidity [4] and is considered to have a crustal origin. In this study, the base cation sum, including $\text{NH}_4^+ \text{-N}$, showed a negative correlation with precipitation, as is common in rainwater events.

The third most abundant anion after Cl^- and SO_4^{2-} was fluoride, with a VWM of $11 \mu\text{eq L}^{-1}$. The fluoride concentration was over $26 \mu\text{eq L}^{-1}$ in more than 28% of events, over $52 \mu\text{eq L}^{-1}$ in 5% of events and over $5 \mu\text{eq L}^{-1}$ in approximately 80% of all events. Fluoride is often related to anthropogenic activities, such as primary aluminum production; fertilizer production [33]; coal combustion; and the production of bricks, tiles, cement, ceramics and glass from materials with high fluoride contents [25]. However, no fluoride was found in rainwater from a coal-fired power plant in Brazil [34] or in two other ecosystems in the northeastern Brazilian Amazon (Amapa State) [35].

The fluoride concentrations found in this study were within the same range as those reported near a fluoride-producing chemical plant in Germany [36]. In 2010 and 2011, Poland Wielkopolski National Park [36], located 12 km from a phosphate fertilizer and a hydrofluoric and sulfuric acid manufacturing plant had similar values as those observed in Barcarena. WALNA et al. [33] linked the high fluoride values found in Poland to emissions from the chemical plants near the sampling sites.

The fluoride VWM in Barcarena ($11 \mu\text{eq L}^{-1}$) was lower than values reported in Xi'an, China ($29 \mu\text{eq L}^{-1}$). As an area highly influenced by fossil fuel combustion and natural soil-derived dust [25], Xi'an is expected to have rainwater with higher fluoride values, especially because a greater rainwater volume falls in the Barcarena area. However, at Barcarena, the maximum fluoride value ($115 \mu\text{eq L}^{-1}$) was greater than the maximum value observed in Xi'an ($60 \mu\text{eq L}^{-1}$). This high value in Barcarena should serve as a warning.

In Barcarena, $\text{NO}_3^- \text{-N}$ and $\text{NH}_4^+ \text{-N}$ VWM values of 6 and $8 \mu\text{eq L}^{-1}$, respectively, were close to values reported in

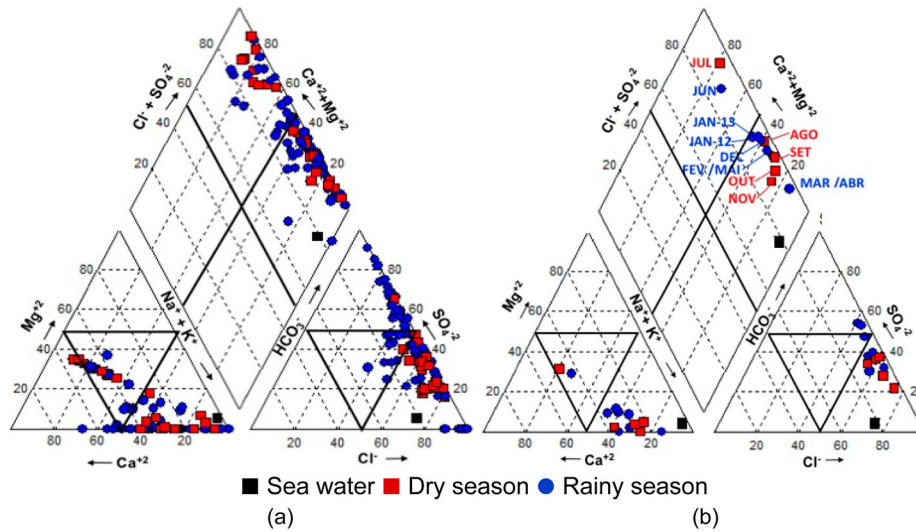


Figure 6. Ternary plots of major ion concentrations ($\mu\text{eq L}^{-1}$) in rainy and dry seasons.

other remote sites in tropical forests ($<7 \mu\text{eq L}^{-1}$) [37]. Despite the similar VWM values of NO_3^- -N and NH_4^+ -N, NH_4^+ -N reached values as high as $166 \mu\text{eq L}^{-1}$, whereas NO_3^- -N only reached values of $33 \mu\text{eq L}^{-1}$. In southern Brazil, such high values were reported only near industrial [38], intensive agricultural and/or urban areas (<7 to $35 \mu\text{eq L}^{-1}$). Both species, NO_3^- -N and NH_4^+ -N, were below the quantification limits ($2 \mu\text{eq L}^{-1}$ and $3 \mu\text{eq L}^{-1}$) in 51% and 76% of the precipitation events, respectively. In the study site, nitrogen species could be related to agricultural soil preparation with fertilizers and biomass burning, which is common in this region, in addition to the continuous sea salt contributions throughout the whole year.

3.4. Ternary plot

Figure 6 shows ternary plots of major ion concentrations in Barcarena rainwater in the dry and rainy seasons. The predominant hydrochemical facies in the rainwater were $\text{Na}^+ + \text{K}^+$ and $\text{Cl}^- + \text{SO}_4^{2-}$, with chemical properties dominated by the seawater contribution and its corresponding dilution line. The ternary plot in Figure 6.b shows the monthly averages. In June and July (dry season), the water samples incorporated Ca^{2+} and SO_4^{2-} , with no carbonate contribution.

3.5. Temporal trends in ion content

The temporal distribution of major ions is presented in Figure 7. Sodium and chloride concentrations show a high significant concentration in August and October 2012 (Figure 7(a)). From August to November 2012, for most ions, the highest concentration was associated

with the lowest precipitation period. This behaviour indicates that the ions were later incorporated into the rain instead of having the same rainwater origin [26]. The monthly concentrations of Ca^{2+} , K^+ , Mg^{2+} and NH_4^+ -N are presented in Figure 7(b). From January to July 2012, a similar trend was identified in K^+ and NH_4^+ -N. Calcium and Mg^{2+} also presented the same trend throughout the whole year with the exception of August 2012 (Figure 7(c)). Figure 7(c) presents the behaviours of SO_4^{2-} _{SS}, F^- , NO_3^- -N, HCO_3^- and SO_4^{2-} _{NSS}. As expected, SO_4^{2-} _{SS} correlates with Cl^- .

3.6. Fraction acidity, ion to ion ratios and enrichment factors

Several authors [24,25,27] presented SO_4^{2-} and NO_3^- -N free anions as the primary acidity source. Therefore, in this work, SO_4^{2-} _{NSS} and NO_3^- -N were compared with H^+ . If all SO_4^{2-} _{NSS} and NO_3^- -N were in free acid forms, the VWM would have been $45 \mu\text{eq L}^{-1}$, and the precipitation pH would have been 4.7 instead of the measured value of 5.8. This pH difference indicates that the precipitation experienced some neutralization and that the components were partially converted to salt. In Barcarena rainwater, the neutralization was mostly performed by cations such as Ca^{2+} , Mg^{2+} , K^+ and NH_4^+ -N. The average FA was 0.08 for the whole collection period, with 90%–95% of acidic species neutralized. Only 15 precipitation events had less than 70% neutralization.

Considering basic species, the NF values for Ca^{2+} , Mg^{2+} , NH_4^+ -N and K^+ were 1.6, 0.8, 0.4 and 0.2, respectively. In the dry season, crustal components are usually responsible for larger neutralization. Indeed, in

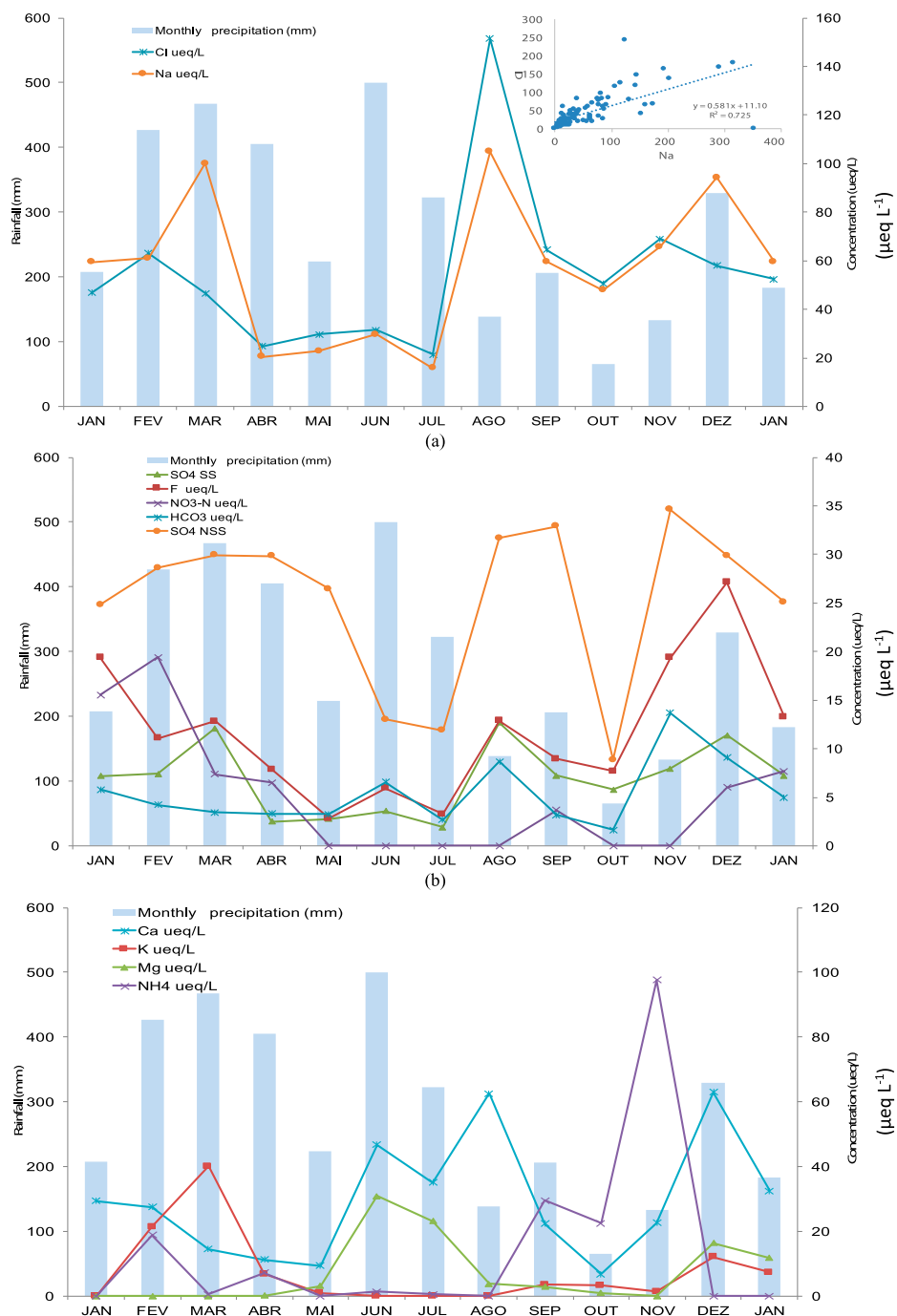


Figure 7. Rainfall (mm) and monthly major ion distributions in Barcarena rainwater ($\mu\text{eq L}^{-1}$).

Barcarena, the NF values for Ca^{+2} , Mg^{+2} and $\text{NH}_4^+\text{-N}$ were greater during the dry season than during the rainy season. The NF for K^+ remained constant, which suggests a different source.

In Barcarena, the $\text{NO}_3^-/\text{SO}_4^{2-}$ ratio ranged from 0.045 (dry season) to 0.185 (rainy season). These low values indicate that most acidity comes from sulfuric acid (82%–95%) instead of nitric acid. A similar $\text{NO}_3^-/\text{SO}_4^{2-}$ ratio was reported close to a coal fired power plant in Filgueira, RS, Brazil (0.189) [26]. Urban centres, with

vehicular sources, have higher ratio values, such as those found in Juiz de Fora, MG (8.33), and in Rio de Janeiro (0.383) [26]. In most cases, SO_2 and NO_x have a common anthropogenic source, and the ratios are not expected to exhibit significant seasonal variation [37]. However, microorganisms can rapidly remove NO_3^- during high-luminosity periods, reducing the $\text{NO}_3^-/\text{SO}_4^{2-}$ ratio during the dry season.

The ratios of Barcarena rainwater ions to Na^+ and to Ca^{+2} and the EFs are presented in Table 2. When an

Table 2. Rainwater components and EFs with respect to seawater and crustal composition.

Seawater Ratio*	Rainwater Ratio*			EF _{seawater} *			%SSF	
	Whole period	Dry season	Rainy season	Whole period	Dry season	Rainy season		
SO ₄ /Na	0.125	1.06	0.64	1.24	9	10	5	11
Cl/Na	1.167	1.071	1.148	1.037	0.92	0.89	0.99	~1
Ca/Na	0.044	0.904	1.132	0.803	21	18	26	5
Mg/Na	0.2253	0.400	0.615	0.305	1.8	1.4	2.7	56
K/Na	0.022	0.164	0.073	0.205	7.5	9.4	3.4	13
NO ₃ /Na	0.00002	0.112	0.029	0.148	5,577	7,411	1,449	0
F/Na	0.00015	0.229	0.208	0.238	1,526	1,587	1,388	0

*Millero et al. [48].

Crustal Ratio*	Rainwater Ratio*			EF _{crust}			%CF	%AF	
	Whole period	Dry season	Rainy season	Whole period	Dry season	Rainy season			
SO ₄ /Ca	0.0188	2.1	1.4	2.4	111	75	126	1	88
Cl/Ca	0.0031	2.8	2.5	2.9	899	820	935	0	0
Mg/Ca	0.561	0.24	0.38	0.18	0.43	0.68	0.31	42	2
K/Ca	0.504	1.1	0.3	1.4	2.1	0.5	2.8	45	42
NO ₃ /Ca	0.0021	0.32	0.04	0.45	154	18	215	1	99
F/Ca	0.0136	0.56	0.54	0.57	41	40	42	2	98

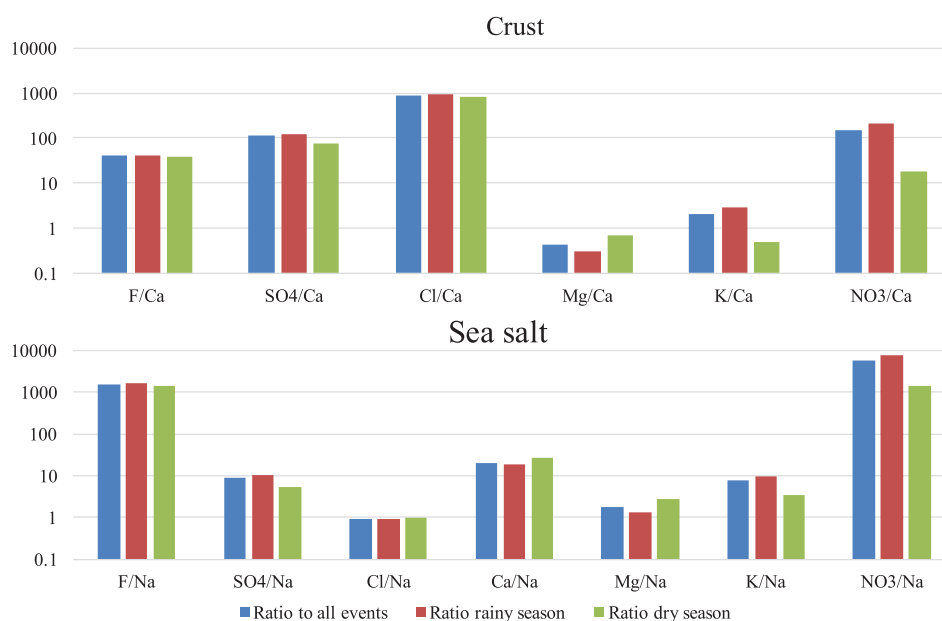
*Lu et al. [30].

EF_{seawater} is close to 1, seawater is considered the most probable source. The same evaluation was performed with Ca⁺² regarding crustal contribution.

The chloride to sodium ratio in Barcarena rainwater was close to the seawater ratio, with a slight decrease during the rainy season. Thus, chloride had a significant marine contribution (SSF ~100%). Fluoride, SO₄⁻² and NO₃⁻-N presented significant enrichment when compared with sea salt and crustal composition. These ions have large anthropogenic contributions. For fluoride, SO₄⁻² and NO₃⁻-N, the AF ranged from 88 to 99%. Potassium was sourced from sea salt (SSF = 13%), crustal (CF = 45%) and anthropogenic contributions (AF = 42%). The anthropogenic potassium source was linked to biomass burning [24].

Figure 8 presents the seasonal change in the ratios of major species to Na and Ca. No seasonal changes were perceived in the F⁻/Na⁺ and F⁻/Ca⁺² ratios, despite the decrease in F⁻ during the dry season. All remaining ions presented some degree of seasonal ratio change (Figure 8). Because similar seasonal trends were identified in SO₄⁻², K⁺ and NO₃⁻-N and in Ca⁺², Mg⁺² and Cl⁻, common sources were attributed to these two groups. Both NF and EF trends indicated that K⁺ has a source component that differs from those of Ca⁺² and Mg⁺², and it is not solely crustal.

Monthly Ca⁺²/Na⁺ and SO₄⁻²/Na⁺ ratios helped to identify changes in the sources as presented in Figure 9. In June and July 2012 (dry season), the Ca⁺²/Na⁺ ratios increased, indicating continental sources

**Figure 8.** Ratios of major ions to Na and to Ca over the whole collection period and in the rainy and dry seasons.

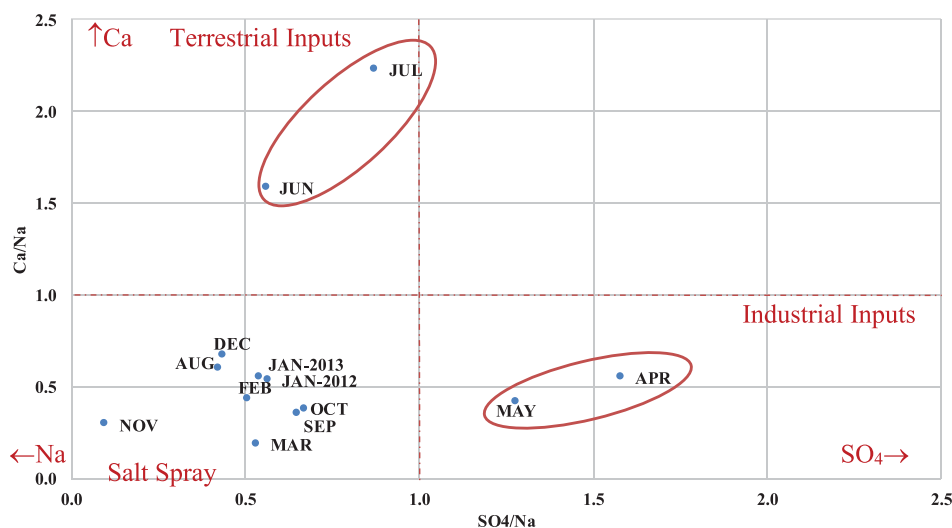


Figure 9. Monthly Ca/Na ratios against SO_4/Na ratios.

Table 3. Principal component factors.

	Factor 1	Factor 2	Factor 3
Collected Volume (ml)	0.9711	0.1116	0.1704
Precipitation (mm)	0.9705	0.1155	0.1724
Na^+	0.7766	0.4986	0.3260
NH_4^+	0.2105	0.1090	0.7734
K^+	0.4751	0.1269	0.8070
Mg^{+2}	0.0128	0.9569	-0.1439
Ca^{+2}	0.4786	0.8558	0.1641
F^-	0.0112	0.8548	0.4082
Cl^-	0.8142	0.4738	0.2934
$\text{NO}_3^- \text{-N}$	-0.1443	0.0398	0.7300
SO_4^{-2}	0.8311	0.3918	0.3784
pH	0.8018	0.0574	-0.1878
H^+	0.6672	-0.2537	0.2013
Bicarbonate	0.9108	0.1364	-0.0588
Eigenvalue	7.7735	2.3875	1.7355
Total Variance%	55.53	17.05	12.40
Cumulative %	55.53	72.58	84.98

[39]. May and April (rainy season) presented a clear increase in industrial sources. During the remaining months, the marine influence was dominant in Barcarena rainwater.

3.7. Probable sources

The sources were evaluated by multivariate statistics with a matrix with 93 cases (rain events) and 14 variables (measured parameters). Ten events were considered outliers and excluded (see supplementary material). Three principal components were found that explained almost 85% of the total variance, as presented in Table 3.

Factor 1 presented good linkage (>0.70) between Na^+ and Cl^- and between SO_4^{-2} and H^+ . These relationships could indicate a combined marine source or later incorporation of SO_4^{-2} , H^+ and CO_2 by clouds. No apparent linkage between SO_4^{-2} and $\text{NO}_3^- \text{-N}$ was present. A

Table 4. Barcarena bulk deposition of major ions in $\text{mg m}^{-2} \text{y}^{-1}$.

Ionic species	Minimum deposition	Maximum deposition
Na^+	1,304	2,378
$\text{NH}_4^+ \text{-N}$	270	380
K^+	650	1,590
Mg^{+2}	225	367
Ca^{+2}	1,040	1,970
F^-	419	479
Cl^-	3,090	3,538
$\text{NO}_3^- \text{-N}$	128	280
SO_4^{-2}	2,385	2,851
Total	14,070	17,890

common source of SO_4^{-2} and $\text{NO}_3^- \text{-N}$ is usually expected from fuel or biomass combustion, as presented [24].

Factor 2 strongly linked (>0.85) to Ca^{+2} , Mg^{+2} and F^- and to a lesser extent Na^+ (0.50). Often Ca is associated with anthropogenic F sources, especially in the aluminum production chain. Cryolite (Na_3AlF_6) is formed by the addition of CaF_2 to reduce the electrolyte melting point [40]. In general, CaF_2 and MgF_2 are found in the electrolyte at levels of 3–7 w/w% and 2–4 w/w%, respectively. Multivariate analysis supports this relationship but EF evaluation was not able to link these elements.

Factor 3 linked $\text{NH}_4^+ \text{-N}$, K^+ and $\text{NO}_3^- \text{-N}$ (>0.70), which could be associated with biomass burning or a fertilizer source. These linkages were not apparent in the EF evaluation but seemed very clear in the PCA.

3.8. Bulk deposition

Table 4 presents the Barcarena deposition range for the most frequent cations and anions. The maximum and minimum deposition rates were related to data completeness. In the minimum deposition calculation, concentrations below the quantification limit were not included. In contrast, the maximum deposition was

calculated as a product of VWM and total precipitation in mm. Therefore, the maximum deposition calculation disregards events with concentrations below the quantification limit, producing higher values.

In 2012, fluoride deposition in Barcarena ranged from 419 to 479 mg m⁻². As a tropical site, fluoride concentrations in Barcarena rainwater were similar those in Poland [36]. However, the higher precipitation in Barcarena leads directly to much greater fluoride deposition. At Wielkopolski National Park, Poland, the fluoride deposition was found as 30.4 mg m⁻² and 45.9 mg m⁻² in 2010 and 2011, respectively [33]. The values found in Poland were related to anthropogenic sources 12 km away, including the Luvena chemical plant that produced fertilizers, hydrofluoric acid and sulfuric acid and had declared fluoride emission values of 19.5 and 2.0 t y⁻¹ in 1988 and 2010, respectively.

In 2012, primary aluminum production worldwide and at Barcarena were 1,985,000 t and 446,000 t respectively [9]. The same year, the worldwide fluoride to air emission was 507 t [9]. Due to the lack of information on Barcarena fluoride emissions, an indirect estimation was made. Barcarena fluoride to air emission was considered a fraction of the worldwide emission at the same ratio as the Barcarena to worldwide aluminum production. Therefore, in this study, the fluoride to air emission budget in 2012 at Barcarena was considered to be 114 t. Considering the county area of 1,311 km² and a one-year period, the theoretical F⁻ deposition rate was estimated to be 87 mg m⁻² y⁻¹. In Barcarena, the measured F⁻ deposition values were found to be greater than the estimated value based on data on the local producer and worldwide emissions.

As presented in Table 5, the SO₄⁻² deposition found in this study was higher than the most robust range proposed by VET et al. in a model for South America [37]. The Barcarena SO₄⁻² values were higher than the value of 498 mg m⁻² y⁻¹ found in Amapa in the 1990s [35]. In Barcarena, the SO₄⁻² deposition values are on the same order of magnitude as sites with high emissions in Bolivia, Chile and Colombia (see Table 5). VET et al. reported low sulfate emission values in coastal areas of Argentina and Amazonia without anthropogenic effects

Table 5. Sulfate emissions in several locations worldwide and in this study [37].

Location	Sulfate mg m ⁻² yr ⁻¹
Bolivia, Chile and Colombia	2,640–3,120
Low-emission areas in Argentina and Amazon	90–120
High-emission areas in South America	600–1,200
Robust range	60–1,890
Coastal zone and Northeast Brazil	300 600
Eastern China	12,000–15,600
Eastern China	6,000–12,000
Present study	2,385–2,851

[37]. The high SO₄⁻² deposition rates found in Barcarena (2,385–2,851 mg m⁻² y⁻¹) were linked to coal burning emissions. In 2012, approximately 650,000 t of coal came through Barcarena harbour solely to heat boilers for the local aluminum producer [41]. According to YOU et al., the sulfur content in coal can range from <0.60% to 3.0%, leading to an estimated sulfate deposition in the Barcarena area ranging from <8,900 mg m⁻² y⁻¹ to 44,600 mg m⁻² y⁻¹ [42]. This process seems to explain the large sulfate deposition found in Barcarena. For further details on this estimation, see the supplementary material.

Barcarena nitrogen deposition varied from 128 to 280 mg m⁻² y⁻¹ as NO₃⁻-N and 270 to 380 mg m⁻² y⁻¹ as NH₄⁺-N. These values seem to agree with the range of 20–200 mg m⁻² y⁻¹ described by VET et al. as low-level deposition, expected in densely populated and/or intensively cultivated areas. Furthermore, these values are still far below the high-level deposition rates that are as high as 2,455 mg m⁻² y⁻¹ commonly observed in several cities in China [37]. The total nitrogen deposition values in Barcarena are less than the value of 1,500 mg m⁻² y⁻¹ reported in Xi'an, China [25], and are similar to the values of 400 mg m⁻² y⁻¹ reported in Venezuela, Colombia, Ecuador, central and southern Brazil, Bolivia, Paraguay, Uruguay and northern Argentina [37].

In this study, NH₄⁺-N, a proxy for N_{reduced}, represented 57–67% of all N deposition, which is compatible with the ratios expected in intensively cultivated areas. In the 1990s, based on modelling, GALLOWAY et al. found that NH₃-N emissions corresponded to 25% of NO_x-N emissions, generally expressed as NO₃⁻-N [43]. In Amapa, from 1993 to 1997 [35], the N deposition was composed of approximately 23% NH₄⁺-N (107 mg m⁻² y⁻¹), with the remaining being NO₃⁻-N (463 mg m⁻² y⁻¹). But as VET et al. reported, the N_{oxidized} values in precipitation decreased for the last 5–10 years with either no reduction or an increase of up to 60–80% in N_{reduced} in certain areas [37]. This pattern also seems to be the case in Barcarena.

Chloride and sodium deposition ranged from 3,090 to 3,538 mg m⁻² y⁻¹ and from 1,304 to 2,378 mg m⁻² y⁻¹, respectively. Based on the model proposed by VET et al., sea salt wet deposition in Barcarena agrees with the expected sea salt deposition range of 2,000–4,000 mg m⁻² y⁻¹ within a distance of 500 km from the Atlantic coast [37]. Barcarena is less than 200 km from the ocean, and sea salt deposition is dependent on the number and size of sea salt particles emitted by breaking waves, which are mainly governed by wave height and wind speed [37].

Base cations, i.e. Ca⁺², Mg⁺², Na⁺ and K⁺, have no gaseous precursors, exist as a relatively constant

proportion in sea salt, can vary greatly in crustal dust, and can also be present in many other natural and anthropogenic sources [37]. In a given area, these species help to reduce any significant acidification effect. In Barcarena, Ca^{+2} deposition ($1,040\text{--}1,970 \text{ mg m}^{-2} \text{ y}^{-1}$) was constant, while K^+ ($650\text{--}1,590 \text{ mg m}^{-2} \text{ y}^{-1}$) and Mg^{+2} ($22\text{--}367 \text{ mg m}^{-2} \text{ y}^{-1}$) were frequently not detected. From July 1993 to June 1997, in Amapa State in Brazil, a geographical area with a similar rainfall trend, presented bulk deposition values for Ca^{+2} , K^+ and Mg^{+2} of 558, 372, and $252 \text{ mg m}^{-2} \text{ y}^{-1}$, respectively [35]. These values seem to agree with the recent Barcarena values. Calcium deposition in Xi'an China was much higher, with values of $4,200 \text{ mg m}^{-2} \text{ y}^{-1}$, because of the high dust occurrence reported in the area [25].

3.9. Recommendations for maintenance teams

As discussed in previous sections, Barcarena rainwater presents clear anthropogenic content due to surrounding industrial activities. Therefore, a change in maintenance procedures to clean and wash electrical components and transmission lines could be required.

In most cases, low-conductivity ($<20 \mu\text{S cm}^{-1}$) groundwater and rainwater could be used to wash critical electrical components. Barcarena rainwater could be a suitable option, as groundwater in the area is not appropriate, with EC values over $50 \mu\text{S cm}^{-1}$ and a high iron content [44]. This study found that in Barcarena, rainwater has average EC values of $15 \pm 15 \mu\text{S cm}^{-1}$. However, high-conductivity events occurred in Barcarena (up to $254 \mu\text{S cm}^{-1}$), which could prevent direct rainwater use without any prior evaluation [45]. In a preliminary evaluation, such EC values correspond to a medium level of site pollution severity with respect to electrical components, based on IEC - 60815-1 and 2 [46,47]. In addition, total rainwater ion deposition values in the range of $14\text{--}17 \text{ g m}^{-2} \text{ y}^{-1}$ could disturb normal operation. The presence of chloride, fluoride, and sulfate can affect the resistance of material to corrosion. By considering this scenario, the following recommendations are proposed for maintenance teams:

- Adopt regular EC monitoring of rainwater events as a fast and reliable indicator of background and especially severe pollution events;
- Schedule preventive maintenance according to seasonal changes;
- Perform site pollution severity evaluations, following IEC - 60815-1 and 2 [46,47], in order to evaluate both soluble and non-soluble contaminants deposited on electrical components;
- Evaluate chloride, sulfate and fluoride concentrations found in electrical components corrosion studies (simulation under high-voltage conditions);
- Consider, according to Barcarena environmental conditions and atmospheric deposition levels, new coatings and protective surfaces, as well as new materials and designs for insulators, upon required electrical component replacement;
- Discuss air monitoring plans and future actions with surrounding companies, customers and city management.

4. Conclusions

In 2012, a rainwater evaluation in Barcarena, Pará, Brazil, was carried out. Acidic compounds were present but neutralized in the majority of precipitation events. Only a few low-pH precipitation events were observed. In these events, a significant amount of SO_4^{-2} and small amounts of F^- , NO_3^- -N and Cl^- were present. In order of VWM abundance, the ions present were $\text{Na}^+ > \text{Cl}^- > \text{SO}_4^{-2} > \text{Ca}^{+2} > \text{K}^+ > \text{F}^- > \text{NH}_4^+$ -N $> \text{Mg}^{+2} > \text{NO}_3^-$ -N. This work identified a clear marine contribution of Na^+ and Cl^- and anthropogenic contributions of SO_4^{-2} , F^- , and NO_3^- . The sulfate source was linked to coal burning. Fluoride, Ca^{2+} and Mg^{2+} were related to the aluminum production chain. Nitrate, K^+ and NH_4^+ presented a mixed source from coal and biomass burning usually associated with fertilizer production. These anthropogenic, marine sea salt and crustal species increased the potential risk of electrical component damage to the power station and transmission lines in Barcarena. Therefore, more attention to electrical component specification, replacement and cleaning procedures are required for the maintenance teams. Further study of the site pollution severity has begun to specifically evaluate directional soluble and non-soluble deposition is recommended for the Barcarena power station. This work started in September 2013 and will be presented elsewhere.

Acknowledgement

Appreciation is extended to all employees of the Vila do Conde Power Station in Barcarena and especially to José Maria Aquino da Luz, Higinio Rodrigues Cardoso and Augusto Sérgio Mourão Noronha. Finally, the authors are grateful to their colleagues of the Centro de Tecnologia da Eletronorte Eletrobras.

Disclosure statement

No potential conflict of interest was reported by the authors.

Funding

The authors thank the financial support provided by Agencia Nacional de Energia Elétrica – ANEEL to the project “Desenvolvimento de Tecnologia para Avaliação de Desempenho de Isoladores e Áreas de Alta Agressividade contrato” #4500078262 from 2013 to 2016, PROPESP/UFPA and National Council for Scientific and Technological Development - CNPq (Grant number 305015/2016-8).

ORCID

Darilena Monteiro Porfírio  <http://orcid.org/0000-0003-3320-0255>

Lucilena Rebêlo Monteiro  <http://orcid.org/0000-0002-4457-4925>

Marcondes Lima da Costa  <http://orcid.org/0000-0002-0134-0432>

References

- [1] Santos P, Otero M, Santos E, et al. Chemical composition of rainwater at a coastal town on Southwest of Europe: what change in 20 years. *Sci Total Environ.* 2011;409:3548–3553.
- [2] Pye K. *Aeolian dust and dust deposits.* Londres: Harcourt Brace Joanovich, Publishers; 1987.
- [3] Pylarinos D, Siderakis K, Pellas I, et al. Assessing pollution of outdoor insulators Cretan power system. *Adv Env Sci Dev Chem.* 2003. Available from: https://talos-ts.com/files/2014_CSCC.pdf
- [4] Lajtha K, Jones J. Trends in cations, nitrogen, sulfate and hydrogen ion concentration in precipitation in the United States and Europe from 1978 to 2010: a new look to an old problem. *Biogeochemistry.* 2013;116:303–334.
- [5] Frontin SD, Maduro-Abreu A, Saavedra AR, et al. *Prospecção e Hierarquização de Inovações Tecnológicas Aplicadas a Linhas de Transmissão.* 1a. Brasília: Teixeira Gáfica e Editores; 2010.
- [6] IBGE - Instituto Brasileiro de Geografia e Estatística. 2016. Available from: <http://cidades.ibge.gov.br/xtras/perfil.php?codmun=150130>.
- [7] Santos LS. *Estudos dos efeitos das descargas atmosféricas nos índices de desempenho das subestações de Vila do Conde e subestação de Marabá [Dissertação de Mestrado].* Belém: ITEC - Programa de Pós-Graduação em Engenharia Elétrica; 2016.
- [8] Norsk Hydro. Annual report; 2016; Oslo Norway.
- [9] Norsk Hydro. Annual report; 2012; Oslo Norway.
- [10] Barros MB. *Mineração, Finanças Públicas e Desenvolvimento Local no Município de Barcarena-PA.* [Dissertação de Mestrado- Instituto de Filosofia e Ciências Humanas-PPGEO]. Belém; 2009.
- [11] INMET - Instituto Nacional de Meteorologia. 2016. Available from <http://www.inmet.gov.br/portal/>.
- [12] Satyamurty P, da Costa CPW, Manzi A. Moisture source for the Amazon Basin: a study of contrasting years. *Theor Appl Climatol.* 2013;111:195–209.
- [13] Pará. *Estatística Municipal de Barcarena.* Secretaria de Planejamento, Orçamento e Finanças, IDESP - Instituto de Desenvolvimento Econômico, Social e Ambiental do Pará; Belém; 2011.
- [14] WMO - World Meteorological Organization. *Manual for the gaw precipitation chemistry programme guidelines, data quality objectives and standard operating procedures No 160.* WMO Edited by Mary A. Allan; 2004.
- [15] Staelens J, Schrijver A, Avermaet P, et al. A comparison of bulk and wet-only deposition in two adjacent sites in Melle (Belgium). *Atmos Environ.* 2005;39:7–15.
- [16] ASTM D1293-18. *Standard test methods for pH of water.* West Conshohocken (PA): ASTM International; 2018.
- [17] ASTM D1125-14. *Standard test methods for electrical conductivity and resistivity of water.* West Conshohocken (PA): ASTM International; 2014.
- [18] ASTM D 6919-17. *Standard test method for determination of dissolved alkali and alkaline earth cations and ammonium in water and wastewater by ion.* West Conshohocken (PA): ASTM International; 2017.
- [19] ASTM D 4327-17. *Standard test method for anions in water by chemically suppressed ion.* West Conshohocken (PA): ASTM International; 2017.
- [20] Alberta Government. *Precipitation chemistry data handling and preparation AEP, air policy, 2015, No. 1.* Edmonton: Alberta Government; 2016.
- [21] Monteiro L, Graffitti D, Albano F, et al. Evaluation of a Brazilian Ion chromatography interlaboratory study. *Accredit Qual Assur.* 2013;18:207–215.
- [22] Øyvind, H. *Paleontological Statistics;* 2015.
- [23] Varejão-Silva MA. *Meteorologia e Climatologia, Versão digital 2 Recife;* 2006.
- [24] Hu G, Balasubramaian R, Wu C. Chemical characterization of rainwater at Singapore. *Chemosphere.* 2003 51:747–755.
- [25] Xiao J. Chemical composition and source identification of rainwater constituents at an urban site in Xi'an. *Environ Earth Sci.* 2016.
- [26] Mimura A, Almeida J, Vaz F, et al. Chemical composition monitoring of tropical rainwater during an atypical dry year. *Atmos Res.* 2016;169:391–399.
- [27] Salve P, Maurya A, Wate S, et al. Chemical composition of major ions in rainwater. *Bull Environ Contam Toxicol.* 2008;80:242–246.
- [28] Moller D. The Na/Cl ratio in rainwater and the seasalt chloride cycle. *Tellus.* 1990;42B:254–262.
- [29] Piñero JM, Rodriguez EA, Perez CM, et al. Influence of marine, terrestrial and anthropogenic sources on ionic and metallic composition of rainwater at suburban site (Northwest coast of Spain). *Atmos Environ.* 2014;88:30–38.
- [30] Lu X, Li Ly, Li N, et al. Chemical characteristics of spring rainwater of Xi'an city, NW China. *Atmos. Environ.* 2011;45:5058–5063.
- [31] Farzaneh M, Chisholm WA. *Insulators for icing and polluted environments.* Piscataway (NJ): IEEE Press Editorial Board; 2009.
- [32] Gao S, Zhou Z, Yang L et al. Factors contributing to haze and the influence on external insulation of power equipments. *Appl Mech Mater.* 2014;700:631–636.
- [33] Walna B, Kurzyca I, Bednorz E, et al. Fluoride pollution of atmospheric precipitation and its relationship with air

- and weather patterns (Wielkopolski National Park, Poland). *Environ Monit Assess.* **2013**;185:5497–5514.
- [34] Flues M, Hama P, Lemes M, et al. Evaluation of the rain-water acidity of a rural region due to coal-fired power plant in Brazil. *Atmo Environ.* **2002**;36:2397–2404.
- [35] Forti CM, Melfi A, Astolfo R, et al. Rainfall chemistry composition in two ecosystems in the northeastern Brazilian Amazon (Amapa State). *J Geophys Res.* **2000**;105:28895–28905.
- [36] Franzaring J, Hrenn H, Schumm C, et al. Environmental monitoring of fluoride emissions using precipitation, dust, plant and soil samples. *Environ Pollut.* **2006**;144(1):158–165.
- [37] Vet R, Artz RS, Carou S, et al. A global assessment of precipitation chemistry and deposition of sulfur, nitrogen sea salt, base cation, organic acids, acidity and pH and phosphorous. *Atmos Environ.* **2014**;93:3–100.
- [38] Casartelli MR, Mirlean N, Peralba MC. An assessment of the chemical composition of precipitation and throughfall in rural-industrial gradient in wet subtropics (southern Brazil). *Environ Monit Assess.* **2008**;144:105–116. doi:10.1007/s10661-007-9949-y.
- [39] Chidambaram S, Paramaguru P, Prasanna MV, et al. Chemical characteristics of coastal rainwater from Puducherry to Neithavasal, Southeastern coast of India. *Environ Earth Sci.* **2014**;72:557–567.
- [40] Fini MF, Soucy G, Désilets M, et al. Sludge formation in hall héroult process: an existing problem. 35th International ICSOBA Conference; 2017; Hamburg, Germany. p. 987–996.
- [41] Barros PHDC. Eficiência na operação do porto de Vila do Conde. Universidade Federal de Santa Catarina; **2013**.
- [42] You CF, Xu XC. Coal combustion and its pollution control in China. *Energy.* **2010**;35(11):4467–4472. doi:10.1016/j.energy.2009.04.019.
- [43] Galloway J, Dentener F, Capone D, et al. Global and regional nitrogen cycles: past, present and future. *Biogeochemistry.* **2004**;70:153–226.
- [44] Piratoba ARA, Ribeiro HMC, Morales GP, et al. Caracterização de parâmetros de qualidade da água na área portuária de Barcarena, PA, Brasil. *Ambient. Água - An Interdiscip. J Appl Sci.* **2017**;12(3):435–456. doi:10.4136/1980-993X.
- [45] Bretuj W, Fleszyński J, Wieczorek K. Influence of composite insulator inclination on its properties degradation in rain conditions. **2011**:4–7.
- [46] IEC - 60815-1. Selection and dimensioning of high-voltage insulators intended for use in polluted conditions - part 1: definitions, information and general principles. Genève: IEC; **2008**.
- [47] IEC - 60815-2. Selection and dimensioning of high-voltage insulators intended for use in polluted conditions - part 2: ceramic and glass insulators for a.c. systems. Genève: IEC; **2008**.
- [48] Millero FJ, Feistel R, Wright DG, et al. The composition of standard seawater and the definition of the reference-composition salinity scale. *Deep-Sea Res.* **2008**;55(1): 50–72.